



# Synthesis, spectroscopic properties, X-ray single crystal analysis and antimicrobial activities of organotin(IV) 4-(4-methoxyphenyl)piperazine-1-carbodithioates

Zia-ur-Rehman<sup>a,b</sup>, Niaz Muhammad<sup>a</sup>, Saqib Ali<sup>a,\*</sup>, Ian S. Butler<sup>b</sup>, Auke Meetsma<sup>c</sup>

<sup>a</sup> Department of Chemistry, Quaid-i-Azam University, Islamabad 45320, Pakistan

<sup>b</sup> Department of Chemistry, McGill University, 801 Sherbrooke St. West, Montreal, Quebec, Canada H3A2K6

<sup>c</sup> Crystal Structure Center, Chemical Physics, Zernike, Institute for Advanced Materials, University of Groningen, Nijenborgh 4, NL-9747 AG Groningen, The Netherlands

## ARTICLE INFO

### Article history:

Received 25 November 2009

Received in revised form 19 May 2011

Accepted 30 June 2011

Available online 12 July 2011

### Keywords:

4-(4-Methoxyphenyl)piperazine-1-carbodithioates  
Organotin(IV) complexes  
NMR spectroscopy  
X-ray diffraction  
Antimicrobial activities

## ABSTRACT

A series of mononuclear organotin(IV) complexes of the types,  $R_3SnL$  { $R = C_4H_9$  (**1**),  $C_6H_{11}$  (**2**),  $CH_3$  (**3**) and  $C_6H_5$  (**4**)},  $R_2SnClL$  { $R = C_4H_9$  (**5**),  $C_2H_5$  (**7**) and  $CH_3$  (**9**)} and  $R_2SnL_2$  { $R = C_4H_9$  (**6**),  $C_2H_5$  (**8**) and  $CH_3$  (**10**)}, have been synthesized, where  $L = 4$ -(4-methoxyphenyl)piperazine-1-carbodithioate. The ligand-salt and the complexes have been characterized by Raman, FT-IR and multinuclear NMR ( $^1H$ ,  $^{13}C$  and  $^{119}Sn$ ) spectroscopy and elemental microanalysis (CHNS). The spectroscopic data substantiate coordination of the ligands to the organotin moieties. The structures of complexes **4** and **6** have been determined by single-crystal X-ray diffraction and illustrate the asymmetric bidentate bonding of the ligand. The packing diagrams indicate  $O\cdots H$  and  $\pi\cdots H$  intermolecular interactions in complex **4** and intermolecular  $S_2C\cdots H$  interactions in complex **6**, resulting in layer structures for both complexes. A subsequent antimicrobial study indicates that the compounds are active biologically and may well be the basis for a new class of fungicides.

© 2011 Elsevier B.V. All rights reserved.

## 1. Introduction

Dithiocarboxylate ligands owe their special significance due to their enormous industrial and biological applications as vulcanization additives, stabilizers for PVC, fungicides, and antibacterial and anticancer agents [1–5]. The diethyldithiocarboxylate anion,  $S_2CNEt_2^-$ , has found extensive clinical use as an antidote for copper poisoning, i.e., Wilson's disease [6], and in ameliorating nephrotoxicity associated with platinum-based chemotherapy [7]. The antibacterial effect of dithiocarboxylates was reported to arise by the reaction of HS-groups with physiologically important enzymes by transferring the alkyl group of the dithioester to the HS-function of the enzyme [8]. Investigations of various types of compounds possessing aminoalkylation ability showed that substituted aminoethyl-N,N-dialkyldithiocarboxylates have cytostatic features presumably via a similar mechanism proposed for antibacterial action [9]. The study of metal complexes containing sulfur donor ligands continues to increase at an unabated pace, chiefly because of their close similarity to several important biomolecules, such as amino acids and vitamins [10]. The synthesis of metal complexes with such types of active ligands is a research area of increased interest to inorganic, pharmaceutical and medicinal chemists as an

approach to the development of new drugs. A judicious choice of ligands can modulate the properties of the complexes produced. As a result, metal-based dithiocarboxylates, such as *ziram* (zinc-dimethyldithiocarboxylate) and *zineb* (zinc ethylene-1,2-bis-dithiocarboxylate) are marketed as fungicides. These are protective fungicides for use on seed foliages and fruit and vegetable crops. The recognition of the importance of Sn–S bond in biology has led to the study of organotin compounds with dithiocarboxylates [11]. Organotin(IV) dithiocarboxylates continue to attract significant attention, again because of their variety of biological applications, such as fungicidal, bactericidal, insecticidal and antitumor activity [12–15]. Moreover, the side-effects, such as localized irritation of the skin with a mild burning sensation and redness and itching, which are associated with commonly used fungicides has led to the search for new fungicides that do not pose serious threats to the environment or to human beings. The coupling of dithiocarbamate ligands with organotin moieties has generated interest because of their dual structure and probable biological applications [16]. We have shown recently that these types of complexes are good DNA binders [17,18]. Because of the broad spectrum of biological properties of dithiocarboxylates and organotin dithiocarboxylates, we thought it would be worthwhile studying the structures and antimicrobial activities of organotin(IV) 4-(4-methoxyphenyl)piperazine-1-carbodithioates and report the results of this investigation here.

\* Corresponding author. Tel.: +92 (051) 90642130; fax: +92 (051) 90642241.

E-mail address: [drsa54@yahoo.com](mailto:drsa54@yahoo.com) (S. Ali).

## 2. Experimental

### 2.1. Materials and methods

Reagents, triorganotin(IV) chlorides, diorganotin(IV) dichlorides and 4-(4-methoxyphenyl)piperazine were obtained from Aldrich Chemical Co., while CS<sub>2</sub> was purchased from Riedal-de Haën. Methanol was dried before use by the literature procedure [19]. Microanalyses were performed using a Leco CHNS 932 apparatus. Infrared spectra were recorded as KBr pellets in the range from 4000–400 cm<sup>-1</sup> on a Bio-Rad Excaliber FT-IR, model FTS 300 MX spectrometer (USA). Raman spectra ( $\pm 1$  cm<sup>-1</sup>) were measured with an InVia Renishaw spectrometer, using argon-ion (514.5 nm) and near-infrared diode (785 nm) laser excitation. WiRE 2.0 software was used for the data acquisition and spectra manipulations. NMR spectra (DMSO-d<sub>6</sub>) were obtained using a Hg-300 MHz spectrometer (<sup>1</sup>H and <sup>13</sup>C) and a Varian Unity 500-MHz instrument [<sup>119</sup>Sn; SnMe<sub>4</sub> (ext) ref.].

#### 2.1.1. Synthesis of 4-(4-methoxyphenyl)piperazinium 4-(4-methoxyphenyl)piperazine-1-carbodithioate (L-salt)

To a 30 mL methanolic solution of 1-(4-methoxyphenyl)piperazine (3 g, 15.6 mmol) was added CS<sub>2</sub> (excess) dropwise with continuous stirring maintained at 0 °C for 0.5 h. The resulting white compound formed (Scheme 1a) was filtered and thoroughly washed with methanol and diethyl ether, and then dried under vacuum. (Yield: 85 %). M. p. 187–189 °C. *Anal. Calc.* for C<sub>23</sub>H<sub>32</sub>N<sub>4</sub>O<sub>2</sub>S<sub>2</sub>: C, 59.97; H, 7.00; N, 12.16; S, 13.92. Found: C, 59.71; H, 6.91; N, 12.12; S, 13.67%. Raman (cm<sup>-1</sup>): 638  $\nu$ (C–S), 1185  $\nu$ (C=S), 1430  $\nu$ (C–N). IR (cm<sup>-1</sup>): 1033  $\nu$ (C–S), 1457  $\nu$ (C–N). <sup>1</sup>H NMR (ppm): 2.91–2.89, 2.48–2.46 (m, 8H, H<sub>2</sub>, 2,2a, 2'a), 4.43–4.40, 3.18–3.17 (m, 8H, H<sub>3</sub>, 3',3a,3'a), 6.92–6.77 (m, 8H, Ar-H), 8.4 (s, 2H, NH<sub>2</sub>). <sup>13</sup>C NMR (ppm): 210.1 (C-1), 48.2, 44.3 (C-2, 2', 2a, 2'a), 50.9, 50.4 (C-3, 3', 3a, 3'a), 152.3, 152.1, 140.5, 140.2, 123.9, 123.4, 121.1, 121.0, 118.4, 118.3, 112.4, 112.1 (Ar-C).

#### 2.1.2. General procedure for the synthesis of complexes

Triorganotin(IV) chloride or diorganotin(IV) dichloride in dry methanol (30 mL) was added dropwise to a ligand-salt in dry methanol (40 mL) in the appropriate molar ratio and the mixture was refluxed for 6 h with constant stirring. The 4-(4-methoxyphenyl)piperazinium chloride was allowed to settle and was removed by filtration. The filtrate was rotary evaporated to afford the desired product, which was then recrystallized from a chloroform-ethanol (3:2) mixture (Scheme 1b). All the complexes are air stable and are soluble in common organic solvents.

**2.1.2.1. Tri(*n*-butyl)tin(IV) 4-(4-methoxyphenyl)piperazine-1-carbodithioate (1).** (Yield: 70%). M.p. 170–171 °C. *Anal. Calc.* for C<sub>24</sub>H<sub>42</sub>N<sub>2</sub>O S<sub>2</sub>Sn: C, 51.71; H, 7.59; N, 5.03; S, 11.50. Found: C, 51.59, H, 7.53, N, 5.00, S, 11.43%. Raman (cm<sup>-1</sup>): 471  $\nu$ (Sn–C), 391  $\nu$ (Sn–S). IR (cm<sup>-1</sup>): 997  $\nu$ (C–S), 1475  $\nu$ (C–N), 510  $\nu$ (Sn–C).

**2.1.2.2. Tricyclohexyltin(IV) 4-(4-methoxyphenyl)piperazine-1-carbodithioate (2).** Yield: 73%. M.p. 144–145 °C. *Anal. Calc.* for C<sub>30</sub>H<sub>48</sub> N<sub>2</sub>O S<sub>2</sub>Sn: C, 56.69; H, 7.61; N, 4.41; S, 10.09. Found: C, 56.58; H, 7.52; N, 4.37; S, 10.03%. Raman (cm<sup>-1</sup>): 484  $\nu$ (Sn–C), 380  $\nu$ (Sn–S). IR (cm<sup>-1</sup>): 1015  $\nu$ (C–S), 1478  $\nu$ (C–N), 502  $\nu$ (Sn–C).

**2.1.2.3. Trimethyltin(IV) 4-(4-methoxyphenyl)piperazine-1-carbodithioate (3).** Yield: 68%. M.p. 162–164 °C. *Anal. Calc.* for C<sub>15</sub>H<sub>24</sub>N<sub>2</sub>O S<sub>2</sub>Sn: C, 41.78; H, 5.61; N, 6.50; S, 14.87. Found: C, 41.64; H, 5.56; N, 6.47; S, 14.77%. Raman (cm<sup>-1</sup>): 507  $\nu$ (Sn–C), 380  $\nu$ (Sn–S). IR (cm<sup>-1</sup>): 1015  $\nu$ (C–S), 1474  $\nu$ (C–N), 530  $\nu$ (Sn–C).

**2.1.2.4. Triphenyltin(IV) 4-(4-methoxyphenyl)piperazine-1-carbodithioate (4).** Yield: 78%. M.p. 136–139 °C. *Anal. Calc.* for C<sub>30</sub>H<sub>30</sub>N<sub>2</sub>O S<sub>2</sub>Sn: C, 58.36; H, 4.90; N, 4.54; S, 10.39. Found: C, 58.22; H, 4.83; N, 4.50; S, 10.33%. Raman (cm<sup>-1</sup>): 269  $\nu$ (Sn–C), 374  $\nu$ (Sn–S). IR (cm<sup>-1</sup>): 1005  $\nu$ (C–S), 1480  $\nu$ (C–N).

**2.1.2.5. Chlorodi-*n*-butyltin(IV) 4-(4-methoxyphenyl)piperazine-1-carbodithioate (5).** Yield: 71%. Sticky material. *Anal. Calc.* for C<sub>20</sub>H<sub>33</sub>N<sub>2</sub>O S<sub>2</sub>SnCl: C, 44.83; H, 6.21; N, 5.23; S, 11.97. Found: C, 44.73; H, 6.17; N, 5.20; S, 11.90%. Raman (cm<sup>-1</sup>): 437  $\nu$ (Sn–C), 388  $\nu$ (Sn–S), 274  $\nu$ (Sn–Cl). IR (cm<sup>-1</sup>): 995  $\nu$ (C–S), 1483  $\nu$ (C–N), 511  $\nu$ (Sn–C).

**2.1.2.6. Di-*n*-butyltin(IV) bis[4-(4-methoxyphenyl)piperazine-1-carbodithioate] (6).** Yield: 75%. M.p. 141–142 °C. *Anal. Calc.* for C<sub>32</sub>H<sub>48</sub>N<sub>4</sub>O<sub>2</sub>S<sub>4</sub>Sn: C, 50.06; H, 6.30; N, 7.30; S, 16.71. Found: C, 49.96; H, 6.23; N, 7.27; S, 16.64%. Raman (cm<sup>-1</sup>): 445  $\nu$ (Sn–C), 376  $\nu$ (Sn–S). IR (cm<sup>-1</sup>): 999  $\nu$ (C–S), 1473  $\nu$ (C–N), 509  $\nu$ (Sn–C).

**2.1.2.7. Chlorodiethyltin(IV) 4-(4-methoxyphenyl)piperazine-1-carbodithioate (7).** Yield: 81%. M.p. 84–86 °C. *Anal. Calc.* for C<sub>16</sub>H<sub>25</sub>N<sub>2</sub>O S<sub>2</sub>SnCl: C, 40.06; H, 5.25; N, 5.84; S, 13.37. Found: C, 39.99; H, 5.23; N, 5.80; S, 13.31%. Raman (cm<sup>-1</sup>): 487  $\nu$ (Sn–C), 383  $\nu$ (Sn–S), 257  $\nu$ (Sn–Cl). IR (cm<sup>-1</sup>): 988  $\nu$ (C–S), 1481  $\nu$ (C–N), 501  $\nu$ (Sn–C).

**2.1.2.8. Diethyltin(IV) bis[4-(4-methoxyphenyl)piperazine-1-carbodithioate] (8).** Yield: 80%. M.p. 138–142 °C. *Anal. Calc.* for C<sub>28</sub>H<sub>40</sub>N<sub>4</sub>O<sub>2</sub>S<sub>4</sub>Sn: C, 47.26; H, 5.67; N, 7.87; S, 18.02. Found: C, 47.16; H, 5.61; N, 7.84; S, 17.95%. Raman (cm<sup>-1</sup>): 497  $\nu$ (Sn–C), 397  $\nu$ (Sn–S). IR (cm<sup>-1</sup>): 978  $\nu$ (C–S), 1475  $\nu$ (C–N), 503  $\nu$ (Sn–C).

**2.1.2.9. Chlorodimethyltin(IV) 4-(4-methoxyphenyl)piperazine-1-carbodithioate (9).** Yield: 82%. M.p. 166–168 °C. *Anal. Calc.* for C<sub>14</sub>H<sub>21</sub>N<sub>2</sub>O S<sub>2</sub>SnCl: C, 37.23; H, 4.69; N, 6.20; S, 14.20. Found: C, 37.13; H, 4.62; N, 6.17; S, 14.13%. Raman (cm<sup>-1</sup>): 530  $\nu$ (Sn–C), 381  $\nu$ (Sn–S), 257  $\nu$ (Sn–Cl). IR (cm<sup>-1</sup>): 977  $\nu$ (C–S), 1485  $\nu$ (C–N), 521  $\nu$ (Sn–C).

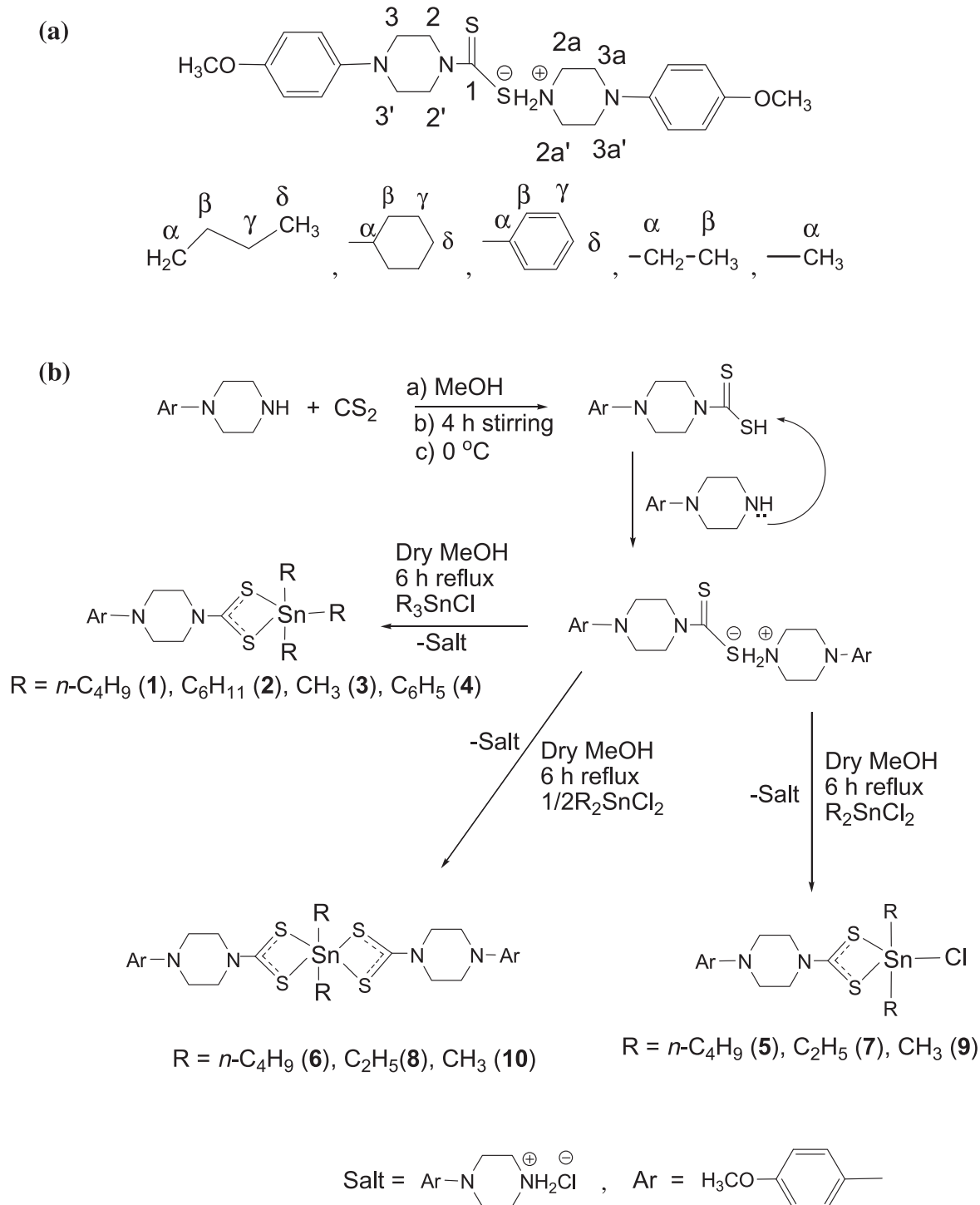
**2.1.2.10. Dimethyltin(IV) bis[4-(4-methoxyphenyl)piperazine-1-carbodithioate] (10).** Yield: 72%. M.p. 174–176 °C. *Anal. Calc.* for C<sub>26</sub>H<sub>36</sub>N<sub>4</sub>O<sub>2</sub>S<sub>4</sub>Sn: C, 45.68; H, 5.31; N, 8.20; S, 18.76. Found: C, 45.59; H, 5.27; N, 8.16; S, 18.67%. Raman (cm<sup>-1</sup>): 507  $\nu$ (Sn–C), 390  $\nu$ (Sn–S). IR (cm<sup>-1</sup>): 989  $\nu$ (C–S), 1474  $\nu$ (C–N), 506  $\nu$ (Sn–C).

#### 2.1.3. X-ray crystallographic studies

The X-ray diffraction data were collected on a Bruker SMART APEX CCD diffractometer, equipped with a 4 K CCD detector. Data integration and global cell refinement was performed with the program SAINT. The program suite SAINTPLUS was used for space group determination (XPREP). The structure was solved by Patterson method; extension of the model was accomplished by direct method and applied to different structure factors using the program DIRDIF. All refinement calculations and graphics were performed with the program PLUTO and PLATON package [20].

#### 2.1.4. Antibacterial activity

The synthesized compounds were tested for antibacterial activity against five different bacterial strains including, *Escherichia coli*, *Salmonella typhi*, *Pseudomonas aeruginosa*, *Staphylococcus aureus*, and *Streptococcus* using the agar well diffusion method [21]. Streptomycin was used as standard drug and the wells (6 mm in diameter) were dug in the media with the help of a sterile metallic borer. Two to eight hours old bacterial inoculums containing approximately 10<sup>4</sup>–10<sup>6</sup> colony forming units (CFU)/mL were spread on the surface of a nutrient agar with the help of a sterile cotton swab.



**Scheme 1.** (a) Numbering scheme for ligand-salt and organic moieties attached to Sn; (b) synthesis of ligand-salt and its organotin(IV) derivatives.

The recommended concentration of the test sample (1 mg/mL in DMSO) was introduced into the respective wells. Other wells supplemented with DMSO and reference antibacterial drug served as negative and positive controls, respectively. The plates were incubated immediately at 37 °C for 20 h. The activity was determined by measuring the diameter of the inhibition zone (in mm), showing complete inhibition. Growth inhibition was calculated with reference to the positive control.

#### 2.1.5. Antifungal activity

The agar tube dilution protocol [21] method was employed to test the antifungal activities of the synthesized compounds against four different strains of fungi, using Clotrimazole as standard drug. Stock solutions of pure compounds (200 µg/mL) were prepared in sterilized DMSO. Sabouraud dextrose agar was prepared by mixing Sabouraud (32.5 g), glucose agar (4%) and agar-agar (20 g) in 500 mL of distilled water followed by dissolution at 90–95 °C on

a water bath. The media (4 mL) was dispensed into screw-capped tubes and autoclaved at 121 °C for 15 min. Known amounts of test compounds were added from the stock solution to non-solidified Sabouraud agar media (50 °C). The contents of the tubes were then solidified at room temperature and inoculated with 4 mm diameter portion of inoculums derived from a 7 days old respective fungal culture. For non-mycelial growth, an agar surface streak was employed. The tubes were incubated at 27–29 °C for 7–10 days and growth in the compound containing media was determined by measuring the linear growth (in mm) and growth inhibition with reference to the respective control.

The inhibition of fungal growth, expressed in percentage terms, was determined using the Vincent equation [22]:

$$\text{Inhibition \%} = 100(C - T)/C$$

where *C* is the diameter of fungal growth for a control and *T* is the diameter of fungal growth for the sample.

### 3. Results and discussion

#### 3.1. Vibrational spectra

In the Raman spectra of the complexes, the presence of a new peak below 400 cm<sup>-1</sup>, attributable to a ν(Sn–S) vibration, signifies coordination of ligand to the organotin moiety. In the chlorodiorganotin derivatives, an additional peak around 260 cm<sup>-1</sup> is observed, which can be assigned to ν(Sn–Cl) stretching, and suggests the substitution of one chloride group during the reactions.

In the IR spectra of organotin(IV) dithiocarbamates, two types of bands have particular structural significance. The first lies in the region 1450–1580 cm<sup>-1</sup>, which is primarily associated with the “thioureide” band due to the ν(N–CSS) vibration; the second, which appears in the region 940–1060 cm<sup>-1</sup>, is associated with a ν(C–S) vibration [23]. In the present study, the N–CSS band was observed at 1457 cm<sup>-1</sup> for the ligand and was shifted appreciably (~20 cm<sup>-1</sup>) upon coordination to the organotin moieties owing to the increase in double bond character of the N–CSS bond [24]. This shift may be due to electron delocalization toward the Sn center. This suggestion is further supported by the shift of the ν(N–CSS) band to still higher energies in the chlorodiorganotin derivatives owing to the presence of the electron-withdrawing chloride group. In all the complexes, the presence of a solitary C–S vibration indicates bidentate coordination of the dithiocarbamate group [25].

#### 3.2. Multinuclear NMR spectra

In the <sup>1</sup>H NMR spectra of the complexes (Table 1), the presence of proton resonances for the ligand moiety as well as for the organotin groups confirmed the formation of the complexes. In every case, the ligand protons appeared as four sets of signals as expected; two multiplets due to the piperazine moiety, a singlet due to the methoxy protons and a multiplet in the aromatic region due to the phenyl ring protons. The proton chemical shift assignments of the methyltin derivatives (**3**, **9** and **10**) is clear-cut from the multiplicity pattern and the <sup>2</sup>J [<sup>119</sup>Sn, <sup>1</sup>H] coupling constants. The C–Sn–C angles, calculated by applying Lockhart's equation [26], given in Table 3, support the tetrahedral, trigonal bipyramidal

**Table 1**  
<sup>1</sup>H NMR data<sup>a,b</sup> of complexes 1–10.

<sup>1</sup> H	(1)	(2)	(3)	(4)	(5)	(6)	(7)	(8)	(9)	(10)
2,2'	3.20–3.14 (m)	3.15–3.12 (m)	3.19 (bs)	3.16–3.13 (m)	3.19–3.16 (m)	3.16–3.13 (m)	3.20–3.16 (m)	3.19–3.16 (m)	3.16–3.13 (m)	3.17 (bs)
3,3'	4.35–4.31 (m)	4.36–4.33 (m)	3.19 (bs)	4.26–4.42 (m)	4.14–4.11 (m)	4.28–4.25 (m)	4.15–4.12 (m)	4.15 (bs)	4.21 (bs)	3.17 (bs)
Ar-H	6.92–6.80 (m)	6.91–6.83 (m)	6.90–6.81 (m)	6.93–6.84 (m)	6.90–6.81 (m)	6.92–6.83 (m)	6.92–6.82 (m)	6.91–6.82 (m)	6.91–6.82 (m)	6.91–6.79 (m)
OCH <sub>3</sub>	3.66 (s)	3.76 (s)	3.76 (s)	3.78 (s)	3.76 (s)	3.77 (s)	3.76 (s)	3.77 (s)	3.76 (s)	3.66 (s)
α	1.63–1.08 (m)	2.02–1.25 (m)	0.65 s [58, 56]	–	1.98–1.31 (m)	2.12–1.38 (m)	1.84 (q)	1.85 (q),(7,8)	1.46 (s) [79]	1.03 (s) [112, 107]
β	1.63–1.08 (m)	2.02–1.25 (m)	–	7.86–7.63 (m)	1.98–1.31 (m)	2.12–1.38 (m)	1.48 (t),(7,5)	1.49 (t),(7,8)	–	–
γ	1.63–1.08 (m)	2.02–1.25 (m)	–	7.47–7.37 (m)	1.98–1.31 (m)	2.12–1.38 (m)	–	–	–	–
δ	0.83 (t),(7,5)	2.02–1.25 (m)	–	7.47–7.37 (m)	0.94 (t),(7,5)	0.94 (t),(6,9)	–	–	–	–

<sup>a</sup>Chemical shift (δ) in ppm. <sup>2</sup>J [<sup>119</sup>Sn, <sup>1</sup>H], <sup>3</sup>J (<sup>1</sup>H, <sup>1</sup>H) in Hz are listed in square brackets and parenthesis, respectively. Multiplicity is given as s = singlet, d = doublet, m = multiplet, bs = broad signal. <sup>b</sup>Numbering in accordance with Scheme 1a.

**Table 2**  
<sup>13</sup>C and <sup>119</sup>Sn NMR data<sup>a,b</sup> of complexes 1–10.

<sup>13</sup> C	(1)	(2)	(3)	(4)	(5)	(6)	(7)	(8)	(9)	(10)
1	197.6	199.2	201.2	196.6	197.4	200.8	197.5	202.4	199.7	190.6
2,2'	43.5	50.7	45.1	50.7	50.6	50.7	50.6	50.6	41	50.6
3,3'	47.6	51.9	50.3	52.5	51.8	51.3	51.8	51.8	47.5	51.3
Ar-C	154.3145.1, 118.7, 115.1	154.6145, 119.114.7	154.7145.4, 119.2114.7	154.8144.7, 119.5114.8	154.8144.4, 119.3114.8	154.7144.9, 119.1114.8	155.4144.4, 119.4,	155.144.8, 119.3114.8	154.2145, 118.7115	154.2144.7, 119.2114.8
OCH <sub>3</sub>	55.8	55.8	55.8	55.8	55.8	55.8	55.7	55.7	55.8	55.7
α	24 [341, 315]	35 [337, 314]	–0.6 [382, 366]	142.4	26.5 [601, 589]	26.6 [787, 771]	21.5 [532, 509]	21.5 [620, 595]	25 [568, 547]	25 [950, 937]
β	28.6 [28.4]	32.3 [17]	–	137	28	34.8	10.4	10.5	–	–
γ	27 [75]	29.5 [67]	–	128.8	27.5	28.8	–	–	–	–
δ	14.4	27.2	–	129.4	13.9	14.1	–	–	–	–
<sup>119</sup> Sn	31.4	–24	–26.6	–181	–191.5	–345	–185	–217.9	–186.6	–238.7

<sup>a</sup> Chemical shifts (δ) in ppm. <sup>η</sup>J [<sup>119</sup>Sn, <sup>13</sup>C] in Hz are listed in square brackets.

<sup>b</sup> Number in accordance with 1a.

**Table 3**  
(C–Sn–C) angles (°) based on NMR parameters of selected complexes.

Compound number	$^1J$ ( $^{119}\text{Sn}$ , $^{13}\text{C}$ ) (Hz)	$^2J$ ( $^{119}\text{Sn}$ , $^1\text{H}$ ) (Hz)	Angle (°)	
			$^1J$	$^2J$
1	341	–	106.6	–
2	337	–	106.3	–
3	382	58	110.2	111.4
5	601	–	129.5	–
6	787	–	145.7	–
7	532	–	123.4	–
8	620	–	131	–
9	568	79	126	124
10	950	112	160	164.6

and octahedral environments around the Sn atoms for complexes **3**, **9** and **10**, respectively. The  $^2J$  [ $^{119}\text{Sn}$ ,  $^1\text{H}$ ] coupling constants for the remaining complexes could not be determined because of their complex multiplet patterns. Trigonal bipyramidal geometry can be proposed for the triphenyltin compound on the basis of the value obtained for the *ortho* protons chemical shift minus those for the *meta* and *para* protons [27].

Clearly resolved  $^{13}\text{C}$  NMR signals were obtained for all the distinct carbon atoms present in the compounds (Table 2). In the ligand, the NCS<sub>2</sub> carbon resonance appeared at about 210.1 ppm, which then shifted upfield in the complexes by ~10 ppm. The upfield shift in the NCS<sub>2</sub> carbon signal is an indication of deshielding of this carbon upon complexation of the ligand to the positive Sn center. In organotinins, the coordination number of the Sn atom can be extracted from the  $^1J$  [ $^{119}\text{Sn}$ ,  $^{13}\text{C}$ ] coupling constant values using Lockhart's equation,  $^1J$  [ $^{119}\text{Sn}$ ,  $^{13}\text{C}$ ] = 11.4 $\theta$  – 875, [28]. The calculated values for complexes **1**, **2** and **3** are 341, 337 and 382 Hz, respectively, characteristic of tetrahedral geometry around Sn [29]. The geometrical assignment for the triphenyltin derivative can be made on the basis of the  $^{13}\text{C}$  chemical shift of the *ipso*-carbon, i.e., 142.4 ppm, which is in accord with trigonal bipyramidal geometry [30]. The  $^1J$  [ $^{119}\text{Sn}$ ,  $^{13}\text{C}$ ] coupling constants indicate five (**5** and **7–9**) and six-coordinated (**6** and **10**) geometry around Sn as shown in Table 3 [31,32].

The  $^{119}\text{Sn}$  NMR chemical shifts for complexes **1**, **2** and **3** are compatible with tetrahedral geometry. Complexes **6** and **10** exhibited  $^{119}\text{Sn}$  NMR signal at –345 ppm, characteristic of a six-coordinate Sn atom. In the rest of the complexes, the  $^{119}\text{Sn}$  values indicate

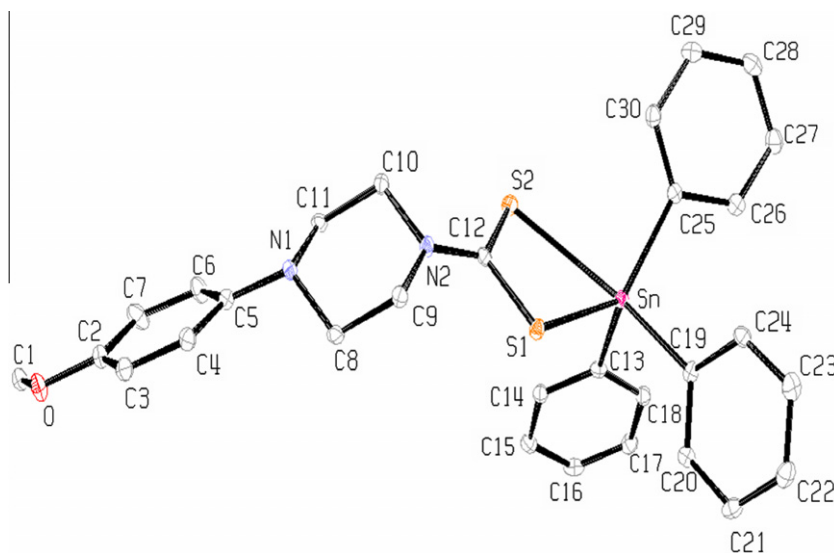
**Table 4**  
Crystal data and structure refinement parameters for compounds **4** and **6**.

	<b>4</b>	<b>6</b>
Empirical formula	C <sub>30</sub> H <sub>30</sub> N <sub>2</sub> OS <sub>2</sub> Sn	(C <sub>16</sub> H <sub>24</sub> N <sub>2</sub> OS <sub>2</sub> ) <sub>2</sub> Sn
Formula mass	617.42	767.74
Crystal system	monoclinic	monoclinic
Space group	<i>P</i> 2 <sub>1</sub> / <i>n</i> , 14	<i>C</i> 2/ <i>c</i> , 15
<i>a</i> (Å)	10.0253(8)	32.768(4)
<i>b</i> (Å)	29.974(2)	6.9313(9)
<i>c</i> (Å)	10.3297(8)	18.877(2)
$\beta$ (°)	117.9951(9)	124.2004(13)
<i>V</i> (Å <sup>3</sup> )	2740.9(4)	3546.0(7)
<i>Z</i> ( <i>Z'</i> )	4 (1)	4 (0.5)
Crystal size (mm)	0.35 × 0.24 × 0.07	0.51 × 0.46 × 0.37
<i>T</i> (K)	100(1)	100(1)
Total reflections	24 147	14 351
Independent reflections all	6767	4040
$\mu$ (Mo K $\alpha$ ) (mm <sup>–1</sup> )	1.111	0.99
For $F_o \geq 4.0 \sigma(F_o)$	5418	3727
$R(F) = \sum( F_o  -  F_c ) / \sum F_o $ For $F_o > 4.0 \sigma(F_o)$	0.0365	0.0267
$wR(F^2) = [\sum[w(F_o^2 - F_c^2)^2] / \sum[w(F_o^2)^2]]^{1/2}$	0.0866	0.0731
Goodness-of-fit (GOF)	1.019	1.077
$\theta$ Range for data collections (°)	2.40–28.28	2.65–27.48
Data/restraints/parameters	6767/0/326	4040/0/197

trigonal bipyramidal geometry in solution. These data are consistent with earlier reports [33].

### 3.3. Crystal structures of compounds **4** and **6**

An ORTEP view of molecule **4**, including the atom numbering scheme, is shown in Fig. 1. Relevant bond lengths and bond angles are collected together in Table 4, while Table 5 summarizes the crystal data. The Sn atom is coordinated by an asymmetrically bound ligand and the  $\alpha$ -carbon atoms of three phenyl groups. The coordination environment is best described as being based on distorted trigonal bipyramidal geometry with the sulfur atom involved in forming the longer Sn...S2 bond occupying one of the axial positions. The geometry around Sn atom can be characterized by the value of  $\tau = (\beta - \alpha)/60$ , where  $\beta$  is the largest of the basal angles around the Sn atom. For compound **4**, this angle is S2–Sn–C19 = 154.67(8)°. The second largest of the basal angles

**Fig. 1.** ORTEP drawing of compound **4** with atomic numbering scheme. All atoms are represented by their displacement ellipsoids drawn at the 50% probability level; hydrogen atoms have been omitted to improve clarity.

**Table 5**  
Selected bond lengths (Å) and bond angles (°) for **4**.

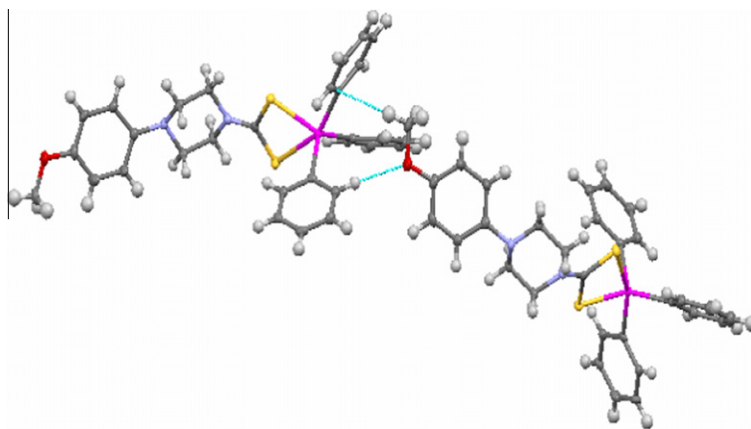
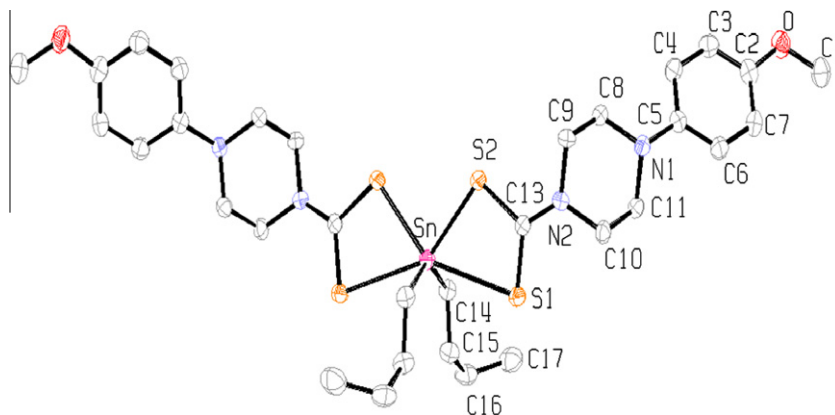
Sn–S1	2.4957(7)	Sn–S2	2.9170(8)
Sn–C13	2.144(3)	Sn–C19	2.170(3)
Sn–C25	2.161(3)	S1–C12	1.758(3)
S2–C12	1.702(3)		
S1–Sn–S2	65.83(2)	S1–Sn–C13	105.49(8)
S1–Sn–C19	90.98(8)	S1–Sn–C25	129.23(9)
S2–Sn–C13	92.39(8)	S2–Sn–C19	154.67(8)
S2–Sn–C25	88.14(8)	C13–Sn–C19	104.09(12)
C13–Sn–C25	119.04(11)	C19–Sn–C25	100.07(11)
Sn–S1–C12	94.49(9)	Sn–S2–C12	81.89(10)
S1–C12–S2	117.80(17)	Sn–C13–C14	121.0(2)
Sn–C13–C18	119.9(2)	Sn–C19–C20	120.0(2)
Sn–C19–C24	121.8(2)	Sn–C25–C26	116.3(2)
Sn–C25–C30	125.8(2)		

**Table 6**  
Selected bond lengths (Å) and bond angles (°) for **6**.

Sn–S1	2.9685(6)	Sn–S2	2.5235(6)
Sn–C14	2.136(3)	Sn–S1a	2.9685(6)
Sn–S2_a	2.5235(6)	Sn–C14a	2.136(3)
S1–C13	1.697(2)	S2–C13	1.743(2)
S1–Sn–S2	64.96(1)	S1–Sn–C14	82.36(6)
S1–Sn–S1a	147.35(2)	S1–Sn–S2a	147.60(2)
S1–Sn–C14a	85.61(6)	S2–Sn–C14	108.09(6)
S2–Sn–S1a	147.60(2)	S2–Sn–S2a	83.01(2)
S2–Sn–C14a	104.34(6)	C14–Sn–S1a	85.61(6)
C14–Sn–S2a	104.34(6)	C14–Sn–C14a	136.24(8)
S1a–Sn–S2a	64.96(1)	S1a–Sn–C14a	82.36(6)
S2a–Sn–C14a	108.09(6)	Sn–S1–C13	80.88(7)
Sn–S2–C13	94.51(7)		

around the Sn atom,  $\alpha$ , for **4** is  $S1-Sn-C25 = 129.23(9)^\circ$ . So the calculated  $\tau$  value for compound **4** is 0.42. Based on the value of  $\tau$ , the structure is biased towards square pyramidal geometry [34]. Presumably, this occurs because of the wide  $S1-Sn-C25$  angle, i.e.,  $129.23(9)^\circ$ , which involves the more tightly bound sulfur atom and the relatively close approach of the less tightly bound sulfur atom, i.e., 2.9170(3) Å. Therefore, the C19 atom of one phenyl group and the S2 of the ligand moiety are in the quasi-axial positions, while the C13 and C25 atoms of the other two phenyl groups and S1 atom are in the planar positions. The sum of the equatorial angles involving the two  $\alpha$ -carbons of the phenyl groups and the

sulfur atom S1 is  $353.7^\circ$ , a marked deviation from the ideal angle of  $360^\circ$ . The unsymmetrical coordination mode of the ligand can also be easily visualized from the two Sn–S bond lengths, the shorter Sn–S1 distance [2.4957(7) Å] and the longer Sn–S2 one [2.9170(8) Å], i.e., a difference of 0.421 Å. The shorter Sn–S bond is close in length to the sum of the covalent radii of Sn and S (2.42 Å), while the longer bond is much shorter than is the sum of the van der Waal's radii of the two atoms (4.0 Å). The S–C bond lengths [ $S1-C12 = 1.758(3)$  Å and  $S2-C12 = 1.702(3)$  Å] also show the anisobidentate nature of the ligand. The packing diagram for complex **4** (Fig. 2) indicates that the molecules are held together through two types of intermolecular interactions, viz.,  $CH_3O \cdots H$

**Fig. 2.** Packing diagram of **4** illustrating  $CH_3O \cdots H$  and  $\pi \cdots H$  intermolecular interactions that are 0.1 Å less than van-der-Waals contacts of the connected atoms.**Fig. 3.** ORTEP drawing of compound **6** with atomic numbering scheme. All atoms are represented by their displacement ellipsoids drawn at the 50% probability level; hydrogen atoms have been omitted to improve clarity.

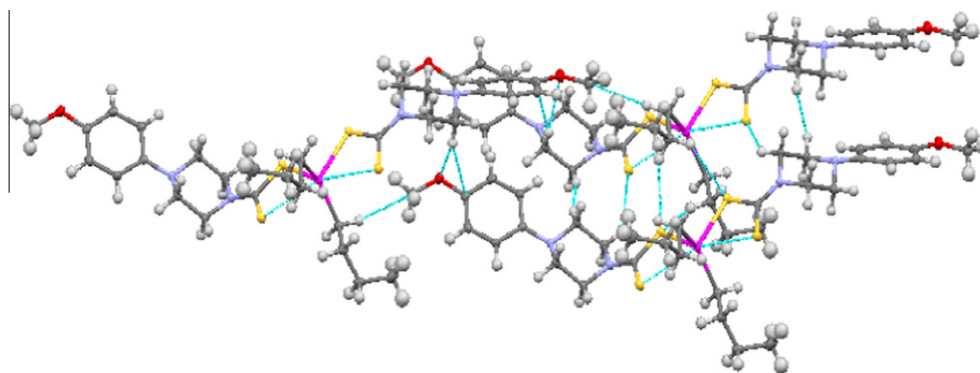


**Fig. 4.** Packing diagram of compounds **6** showing intermolecular  $S_2C\cdots H$  and  $CH_3O\cdots H$  interactions that are 0.1 Å less than van-der-Waals contacts of the connected atoms.

and  $\pi\cdots H$  interactions. These interactions are weak and are less than the van der Waal's radii of the connected atoms by 0.1 Å.

The structure of compound **6** is shown in Fig. 3. Crystal data and selected interatomic parameters are presented in Tables 4 and 6, respectively. The Sn atom is coordinated by two butyl groups and two 4-(4-methoxyphenyl) piperazine-1-carbodithioate ligands, with the latter adopting similar behavior in coordination modes. The two dithiocarboxylate ligands are anisobidentically chelated to Sn, with one long and one short Sn–S bond ( $\text{av} = 2.9685(6)$  Å and  $2.5235(6)$  Å, respectively). The longer Sn–S distances are significantly less than is the sum of the van der Waal's radii (4.0 Å), and the coordination number of Sn is, however, unambiguously assigned as six. The overall geometry at Sn is, however, highly distorted from *trans* octahedral: the C–Sn–C angle is only  $136.24(8)^\circ$ , and the Sn and four  $NCS_2$  sulfur atoms of the

dithiocarboxylate ligands are nearly coplanar but are badly distorted from square-planar geometry [*cis* S–Sn–S angles range from  $64.96(1)^\circ$  to  $147.60(2)^\circ$ ]. In both anisobidentate ligands, each short Sn–S bond is associated with a long C–S bond and vice versa; this is with a consequence of the bonding asymmetry of the ligands. The bond angles subtended at the Sn atom by the methylene carbons and S2 and S2a atoms range from  $108.09(6)^\circ$  to  $104.34(6)^\circ$  demonstrating that the Sn–C bonds are bent toward the longer Sn–S bonds. This is obviously a result of repulsion between the bonding electron pairs around the central Sn atom. Electronic and steric arguments have also been invoked to account for the distortion of similar structures from the regular octahedral geometry. Thus, the coordination geometry about the Sn atom in compound **6** is best described as being distorted skew trapezoidal-bipyramidal. The geometry and bond lengths of  $SnC_2S_4$  core are comparable

**Table 7**  
Antibacterial activity data of ligand and its organotin(IV) derivatives.<sup>a,b</sup>

Bacterium	Clinical implication	Zone of Inhibition (mm)										Ref. Drug	
		L-salt	(1)	(2)	(3)	(4)	(5)	(6)	(7)	(8)	(9)		(10)
<i>Escherichia coli</i>	Infection of wounds, urinary tract and dysentery	29	30	12	21	28	23	22	30	26	22	20	34
<i>Salmonella typhi</i>	Typhoid fever, localized infection	18	30	22	25	28	29	24	31	31	24	19	31
<i>Pseudomonas aeruginosa</i>	Infection of wounds, eyes, septicemia	8	14	3	23	6	16	13	23	20	19	15	24
<i>Staphylococcus aureus</i>	Food poisoning, scaled skin syndrome, endocarditis	9	4	6	22	5	25	24	28	26	24	16	38
<i>Streptococcus</i>	Strep throat	30	31	0	30	30	23	26	30	28	18	18	38

<sup>a</sup> *In vitro*, agar well diffusion method, conc. 1 mg/mL of DMSO.

<sup>b</sup> Reference drug, Streptomycin.

**Table 8**  
Antifungal activity<sup>a</sup> of ligand and its organotin(IV) derivatives.

Sample	Tested fungi							
	<i>Aspergillus niger</i>		<i>Aspergillus flavus</i>		<i>Helminthosporium solani</i>		<i>Alternaria solani</i>	
	Linear growth	% Inhibition	Linear growth	% Inhibition	Linear growth	% Inhibition	Linear growth	% Inhibition
Control <sup>b</sup>	85	–	86	–	87	–	90	–
L-salt	16	81.2	86	0.0	12	86.2	10	88.9
(1)	54	36.5	10	88.4	10	88.5	12	86.7
(2)	20	76.5	61	29.1	69	20.7	80	11.1
(3)	13	84.7	20	76.7	83	4.6	83	7.8
(4)	41	51.8	10	88.4	12	86.2	11	87.8
(5)	76	10.6	81	5.8	80	8.0	80	11.1
(6)	51	40.0	81	5.8	77	11.5	60	33.3
(7)	83	2.4	86	0.0	78	10.3	79	12.2
(8)	44	48.2	86	0.0	78	10.3	51	43.3
(9)	73	14.1	82	4.7	86	1.1	80	11.1
(10)	16	81.2	86	0.0	79	9.2	40	55.6
Clotrimazole	60	29.4	86	39.5	51	41.4	48	46.7

<sup>a</sup> Concentration: 200 µg/mL of DMSO.

<sup>b</sup> Control = DMSO.

with those that are usually observed for most octahedral complexes [35,36]. An analysis of the crystal packing for this compound (Fig. 4) shows that the molecules are held together by  $S_2C \cdots H$  and  $CH_3O \cdots H$  interactions, that are 0.1 Å less than van-der-Waals contacts of the connected atoms. No secondary  $Sn \cdots S$  interactions are noted, as is usually the case for monoclinic forms of diorganotin(IV) dithiocarboxylates [12].

### 3.4. Antibacterial and antifungal activities

The antibacterial activities of ligand-salt and complexes were tested by agar well diffusion method [21] against five different strains of bacteria are shown in Table 7. The ligand-salt and the complexes exhibited good activities against the test bacteria. The organotin derivatives are more active than is the ligand-salt. i.e., complexation increases the bactericidal potency. This situation can be understood in term of chelation theory, which states that the polarity of the metal ion is reduced upon complexation, which results in an increase of the lipophilicity of the metal complexes, thus facilitating their ability to cross the cell membrane more easily [37]. Among the triorganotin(IV) derivatives examined here, the bactericidal activities of complexes **1**, **3** and **4** are fairly good. Complex **1** exhibited lower activity against *S. aureus* and *Streptococcus*. Complex **2** is the least active, while complex **3** is active against all the bacterial strains. In general, the chlorodiorganotin(IV) complexes are more active than are their counterparts without chloride substituents. The most probable reason is that chloro group might decrease the hydrophobic character of the complexes, rendering them biologically active [38]. In order to check the idea whether the precursors, organotin(IV) chloride, are more or less active than the corresponding organotin(IV) derivatives of the ligand; we select  $(C_6H_5)_3SnCl$ ,  $(CH_3)_3SnCl$ ,  $(CH_3)_2SnCl_2$  and  $(C_2H_5)_2SnCl_2$ , and screened them against *E. coli*. The zone of inhibition of the precursors is 10, 15, 50 and 34 mm, respectively. The activity of  $(C_6H_5)_3SnCl$  and  $(CH_3)_3SnCl$  is less than their corresponding triorganotin(IV) derivatives of the ligand, whereas as for the other two precursors the case is reversed. By comparing antibacterial results of our compounds with the previously reported organotin(IV) compounds [39,40] show the supremacy of the former.

The agar tube dilution protocol [21] method was employed to test the antifungal activities of the synthesized compounds against four different strains of fungi, and the results are shown in Table 8. The triorganotin(IV) derivatives are more active than are the chlorodi- and diorganotin(IV) complexes against the fungi tested. In fact, the activity of the triorganotin(IV) complexes is even more than that of the standard drug. The cytoplasmic membrane may be a possible target of action. Interaction of complexes alters the membrane fluidity [41] and the organism dies because of extensive  $K^+$  leakage. The ligand-salt employed in the present work and the resulting complexes, **1**, **2**, **3** and **4**, may represent a new class of drugs that can be administered alone or in combination with others in current use, as new formulations for fungal diseases.

The  $(C_4H_9)_3SnCl$ ,  $(C_6H_5)_3SnCl$ ,  $(C_6H_{11})_3SnCl$  and  $(C_4H_9)_2SnCl_2$  were tested against *Aspergillus niger* and the % inhibition was found to be 50, 20, 10 and 15, respectively. Compound **2**, **4** and **6** are more active than their respective precursors. Our antifungal results supersede the findings of Singh et al. for the other organotin compounds [42].

## 4. Conclusions

The present paper describes the synthesis, characterization and antimicrobial activities of ten new organotin(IV) 4-(4-methoxyphenyl)piperazine-1-carbodithioates. X-ray single crystal study proved a dimeric and a supramolecular molecular structure for

complexes **4** and **6** with a distorted square pyramidal and a skew-trapezoidal geometry, respectively.

The square-pyramidal geometry is unique because this kind of geometry is not previously reported in the literature for triphenyltin(IV) derivatives. The antimicrobial activities of the complexes are, in broad terms, excellent and far exceed the level for the ligand-salt. The influence of the tin is clearly visible in the antibacterial activity. Such a study will be helpful in designing novel antifungal metal-based drugs.

## Acknowledgements

We thank the Higher Education Commission of Pakistan and the NSERC (Canada) for financial support.

## References

- [1] G. Faraglia, S. Sitran, D. Montagner, *Inorg. Chim. Acta* 358 (2005) 971.
- [2] O. Guzel, A. Salman, *Bioorg. Med. Chem.* 14 (2006) 7804.
- [3] P.J. Heard, *Prog. Inorg. Chem.* 53 (2005) 1.
- [4] G.D. Thorn, R.A. Ludwig, *The Dithiocarbamates and Related Compounds*, Elsevier, Amsterdam, 1962.
- [5] F.W. Sunderman, *Ann. Clin. Lab. Sci.* 9 (1979) 1.
- [6] G.Y. Ding, R.T. Li, *Bioorg. Med. Chem. Lett.* 15 (2005) 1915.
- [7] D.L. Bodenner, P.C. Dedon, P.C. Keng, R.F. Borch, *Can. Res.* 46 (1986) 2745.
- [8] A.H. Neims, D.S. Coffey, L. Helleman, *J. Biol. Chem.* 241 (1966) 5941.
- [9] S. Khan, S.A.A. Nami, K.S. Siddiqi, *J. Organomet. Chem.* 693 (2008) 1049.
- [10] L.A. Komarnisky, R.J. Christopherson, *Nutrition* 19 (2003) 54.
- [11] S. Ozkirimli, T.I. Apak, M. Kiraz, Y. Yegenoglu, *Arch. Pharm. Res.* 28 (2005) 1213.
- [12] E.R.T. Tiekink, *Appl. Organomet. Chem.* 22 (2008) 533.
- [13] H.P. Chauhan, N.M. Shaik, *J. Inorg. Biochem.* 99 (2005) 538.
- [14] G. Eng, X. Song, Q. Duong, D. Strickman, J. Glass, L. May, *Appl. Organomet. Chem.* 17 (2003) 218.
- [15] H.D. Yin, S.C. Xue, *Appl. Organomet. Chem.* 20 (2006) 283.
- [16] E.R.T. Tiekink, *Appl. Organomet. Chem.* 22 (2008) 533.
- [17] Z. Rehman, A. Shah, N. Muhammad, S. Ali, R. Qureshi, I.S. Butler, *Eur. J. Med. Chem.* 44 (2009) 3986.
- [18] Zia-ur-Rehman, A. Shah, N. Muhammad, S. Ali, R. Qureshi, I.S. Butler, *J. Organomet. Chem.* 694 (2009) 1998.
- [19] W.F.L. Armarego, C. Chai, *Purification of Laboratory Chemicals*, fifth ed., Butterworth, Oxford, 2003.
- [20] A.L. Spek, PLATON (Version of October 2007), Program for the Automated Analysis of Molecular Geometry (A Multipurpose Crystallographic Tool), University of Utrecht, The Netherlands, *J. Appl. Crystallogr.* 36 (2003) 7.
- [21] A. Rehman, M.I. Choudhary, W.J. Thomsen, *Bioassay Techniques for Drug Development*, Harwood Academic Publishers, The Netherlands, 2001, p. 14.
- [22] J.M. Vincent, *Nature* 189 (1947) 850.
- [23] L. Ronconi, L. Giovagnini, C. Marzano, F. Bettio, R. Graziani, G. Pilloni, D. Fregona, *Inorg. Chem.* 44 (2005) 1887.
- [24] L. Ronconi, C. Maccato, D. Barreca, R. Saini, M. Zancato, D. Fregona, *Polyhedron* 24 (2005) 521.
- [25] F. Bonati, R. Ugo, *J. Organomet. Chem.* 10 (1967) 257.
- [26] T.P. Lockhart, W.F. Manders, E.M. Holt, *J. Am. Chem. Soc.* 108 (1986) 6611.
- [27] S. Shahzadi, S. Ali, K. Wurst, M.N. Haq, *Heteroat. Chem.* 18 (2007) 664, and references therein.
- [28] T.P. Lockhart, W.F. Manders, E.M. Holts, *J. Am. Chem. Soc.* 108 (1986) 6611.
- [29] R. Willem, A. Bouhdid, M. Biesemans, J.C. Martins, D. Vos, E.R.T. Tiekink, M. Gielen, *J. Organomet. Chem.* 514 (1996) 203.
- [30] T.S.B. Baul, S. Dhar, S.M. Pyke, E.R.T. Tiekink, E. Rivarola, R. Butcher, F.E. Smith, *J. Organomet. Chem.* 633 (2001) 7.
- [31] B. Wrackmeyer, *Annu. Rep. NMR Spectrosc.* 16 (1985) 73.
- [32] B. Wrackmeyer, *Annu. Rep. NMR Spectrosc.* 38 (1999) 203.
- [33] A. Tarassoli, T. Sedaghat, B. Neumüller, M. Ghassemzadeh, *Inorg. Chim. Acta* 318 (2001) 15.
- [34] A.W. Addison, T.N. Rao, J. Reedijk, J. van Rijn, G.C. Verschoor, *J. Chem. Soc., Dalton Trans.* (1984) 1349.
- [35] M.I. Mohamed-Ibrahim, S.S. Chee, M.A. Buntine, M.J. Cox, R.T. Tiekink, *Organometallics* 19 (2000) 5410.
- [36] Zia-ur-Rehman, S. Ali, N. Muhammad, A. Meetsma, *Acta Crystallogr., Sect. E* 63 (2007) m431.
- [37] C.M. Thimmaiah, G.T. Chadrapa, W.D. Lloyd, *Inorg. Chim. Acta* 107 (1985) 281.
- [38] D.C. Menezes, F.T. Vieira, G.M. de Lima, J.L. Wardell, M.E. Cortés, M.P. Ferreira, M.A. Soares, A. Vilas Boas, *Appl. Organomet. Chem.* 22 (2008) 221.
- [39] M. Affan, S.W. Foo, I. Jusoh, S. Hanapi, E.R.T. Tiekink, *Inorg. Chim. Acta* 362 (2009) 5031.
- [40] W. Kang, X. Wub, J. Huang, *J. Organomet. Chem.* 694 (2009) 2402.
- [41] Zia-ur-Rehman, N. Muhammad, S. Ali, I.S. Butler, A. Meetsma, M. Khan, *Polyhedron* 28 (2009) 3439.
- [42] R.V. Singh, P. Chaudhary, K. Poonia, S. Chauhan, *Spectrochim. Acta Part A* 70 (2008) 587.